











FRESH-Printing of a Multi-actuator Biodegradable Robot Arm for Articulation and Grasping

Avery S. Williamson¹ , Wenhuan Sun¹ , Ravesh Sukhnandan¹ , Brian Coffin² ,
Carmel Majidi¹ , Adam Feinberg^{2,3} , Lining Yao⁴ ,
and Victoria A. Webster-Wood^{1,2,5} 

¹ Department of Mechanical Engineering, Carnegie Mellon University, Pittsburgh, PA 15218, USA

vwebster@andrew.cmu.edu

² Department of Biomedical Engineering, Carnegie Mellon University, Pittsburgh, PA 15218, USA

³ Department of Materials Science and Engineering, Carnegie Mellon University, Pittsburgh, PA 15218, USA

⁴ Human-Computer Interaction Institute, School of Computer Science, Carnegie Mellon University, Pittsburgh, PA 15218, USA

⁵ McGowan Institute for Regenerative Medicine, Carnegie Mellon University, Pittsburgh, PA 15218, USA

<http://engineering.cmu.edu/borg>

Abstract. The recent popularity of soft robots for marine applications has established a need for the reliable fabrication of actuators that enable locomotion, articulation, and grasping in aquatic environments. These actuators should also reduce the negative impact on sensitive ecosystems by using biodegradable materials such as organic hydrogels. Freeform Reversible Embedding of Suspended Hydrogels (FRESH) printing can be used for additive manufacturing of small-scale biologically derived, marine-sourced hydraulic actuators by printing thin-wall structures out of sustainably sourced calcium-alginate hydrogels. However, controlling larger alginate robots with complex geometries and multiple actuation mechanisms remains challenging due to the reduced strength of such soft structures. For tethered hydrogel hydraulic robots, a direct interface with fluid lines is necessary for actuation, but the drag forces associated with tethered lines can quickly overcome the actuation force of distal and extremity structures. To overcome this challenge, in this study, we identify printing parameters and interface geometries to allow the working fluid to be channeled to distal components of FRESH-printed alginate robots and demonstrate a proof-of-concept biodegradable robotic arm for small object manipulation and grasping in marine environments.

Keywords: 3D printing · Hydrogel actuators · Biodegradability · Sustainability · Shape morphing · Soft robotics

Supplementary Information The online version contains supplementary material available at https://doi.org/10.1007/978-3-031-38857-6_10.

1 Introduction

Soft robots have broad applications in human and environmental monitoring due to their ability to interact more safely with organisms than their traditional rigid counterparts [1]. Compliant actuators have seen broad adoption in wearable devices [2–4], swimming [5–11, 33] and crawling robots [10–13], grippers [14, 15], and tentacles [15, 33]. Recently, many researchers have endeavored to move their robotic systems beyond the lab, deploying robotic devices capable of adapting to locomotion in both amphibious and terrestrial environments [9–11, 16, 34].

However, many of the materials used in soft robotics may pose risks to fragile marine ecosystems. Most conventional soft robot materials rely on plastics and elastomers [17]. These may bioaccumulate in coastal ecosystems if robotic systems fail during deployment. Furthermore, small-scale marine robots may be accidentally ingested by native life [18, 19]. In particular, turtles, petrels, and other marine life can experience strongly adverse outcomes from ingesting non-digestible materials [18–21].

Biologically sourced and biodegradable materials are of growing interest in soft robotics to help minimize the risk of deploying soft robots in sensitive environments [1, 8, 11, 15, 17]. Biologically sourced actuators can span a spectrum from bio-derived plastic devices [23–25] to biotic muscle-based actuators [5, 12, 13]. Using plant-derived materials, researchers have developed pneumatic [26] and electrohydraulic [27] actuators that can biodegrade in natural environments. However, these actuators have been primarily tested in air. Biohybrid actuators that incorporate natural muscle tissue can operate in aquatic and marine ecosystems depending on the cell or tissue type [9–11, 16]. However, the metabolic and environmental conditions must be precisely regulated to maintain functionality, which currently prevents deployment outside of a research laboratory.

For marine applications, we have recently demonstrated that biodegradable, biologically sourced hydraulic actuators can be fabricated using Freeform Reversible Embedding of Suspended Hydrogels (FRESH) [15, 28]. These structures maintain functionality with minimal loss in range of motion over 100s of cycles, then degrade completely within a week of incubation on an ambient marine environment. FRESH enables the direct 3D printing of biologically relevant hydrogel inks featuring hydrophilic, porous, polymer networks. This printing method expands the geometric design freedom of printed structures and allows for more complex geometries to be fabricated than with methods such as casting that require removal from a mold or post-casting assembly [15]. In this way, FRESH-printing is advantageous over alternative manufacturing methods. Common printing materials include alginate, fibrin, collagen type I, and Matrigel [28]. For marine applications, alginate, a polysaccharide derived from seaweed that is naturally biodegradable, is compatible with FRESH printing [29]. Alginate can be ionically cross-linked using multivalent cations (e.g., Ca^{2+}), resulting in a physical gel with tunable mechanical properties [22]. Using biologically derived alginate hydrogel inks, we have previously created proof-of-concept demonstrations for bending and linear actuators, small-scale robotic grippers, and multi-actuator structures for end-effector positioning. These actuators are fully biodegradable, can undergo reversible shape and stiffness morphing, and are safely edible by marine organisms [15]. Whereas this prior work demonstrated that FRESH-printed alginate actuators were reliable, biodegradable, and even

edible, all actuators were interfaced with driving syringe pumps at a single fixed base. Our prior preliminary attempts to interface more distal actuators on complex structures with independent tubing found that the actuators could not overcome the tube stiffness, which greatly restricted motion.

To overcome this limitation, in this work, we present the application of FRESH printing to larger, multi-actuator biodegradable robots with internal fluidic routing for independent control of distal actuators. We tested the ability of FRESH printing to create straight and angled fluidic channels using an alginate bioink and identified channel geometries needed for perfusion (Fig. 2H, 3A). Additionally, we designed, printed, and tested a proof-of-concept robotic arm with four degrees of freedom for end effector positioning and independent control of a distal soft grasper via internal routing. To our knowledge, this proof-of-concept work presents the first 3D-printed biodegradable robotic arm created using biologically sourced marine-derived materials.

2 Experimental Materials and Methods

Materials. Sodium alginate (mannuronic to guluronic acid (M/G) ratio = 1:3, Allevi), Alcian Blue (Alfa Aesar), gelatin Type B (Fisher Chemical), Pluronic F-127 (Sigma-Aldrich), gum arabic (Sigma-Aldrich), hydrochloric acid (HCl) (1N, Fisher Chemical), calcium chloride (CaCl_2) (Fisher Chemical), water-resistant glue (Ultra-Gel Control Super Glue, Loctite) were used as received.

2.1 Alginate Bioink Preparation

Preparation of the alginate bioink was performed as previously described [15]. Briefly, the alginate bioink was prepared by solubilizing sodium alginate powder in heated (65 °C) deionized water to a concentration of 4% w/v and mixing using a magnetic stirrer. Alcian Blue powder was added to the bioink at a concentration of 0.02% (w/v) to allow the hydrogel to be visible during testing.

2.2 Preparation of Gelatin Support Bath

The gelatin support bath was prepared following previous work [15, 29–31]. Briefly, 2.0% (w/v) gelatin Type B, 0.25% (w/v) Pluronic F-127, and 1.0% (w/v) gum arabic were thoroughly mixed in 50% (v/v) ethanol solution at 70–80 °C using magnetic stirring. The solution was adjusted to 5.55–5.57 pH by adding 1N HCl dropwise while monitoring pH with a benchtop pH meter (Apera Instruments). This precursor solution was stirred overnight in a temperature-controlled room (21–24 °C) using an overhead stirrer at 550–575 rpm. After stirring, the gelatin slurry was washed three times with 0.1% (w/v) CaCl_2 . Finally, the slurry solution was diluted to a concentration of 0.05% (w/v) CaCl_2 , vortexed, centrifuged at 2000 g for 5 min immediately before printing.

2.3 FRESH Printing of Alginate Robot Components

Methods for modeling, slicing, and printing alginate robots were adapted from Sun et al. [15] and prior literature [29–31] (Fig. 1). Briefly, all digital models in this study were created using Solidworks (Dassault Systèmes) and converted to Geometric codes (G-code) using Slic3r (<http://slic3r.org>) (16 mm/s print speed, 50 μm layer height). Perimeter-only features were used through the walls of the structure. A full slicer configuration profile is accessible in the supplemental materials.

All 3D printing was performed using a Replistruder V4 on a desktop CoreXY 3D printer (Elf, Creativity Technology). A 5 mL gastight syringe (Model 1005TLL, Hamilton) with a G30 blunt-tip needle (DN-05-LP-30, Bestean) was loaded with the bioink before printing, and excess air bubbles were expelled. Printing wells were vacuum formed from thermoplastic polycarbonate material to house the gelatin slurry suspension and fixed to the printer bed with double-sided tape (Fig. 1A). For structures less than 30 mm in the z direction, the 1-inch G30 needle was attached directly to the Hamilton syringe via a Luer-lock connection. A compound needle was fabricated to achieve printed structures exceeding 30 mm by inserting a 1-inch G30 needle into the open end of a 1-inch G23 needle via a press fit and connecting to the Hamilton syringe via a Luer-lock connection on the G23 needle.

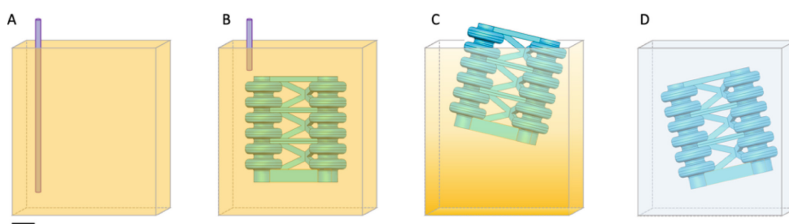


Fig. 1. FRESH-printing process of a typical alginate structure. (A) Gelatin slurry filled printing well with a G30 needle represented in purple. (B) Newly printed structure incubating in slurry at room temperature. (C) Slurry liquefaction in 37 °C water bath and released printed structure. (D) Retrieved part in fresh 2.5% (w/v) CaCl_2 solution.

During printing, alginate structures were crosslinked by the 0.05% (w/v) CaCl_2 remaining in the slurry to ensure filament fusion and increase hydrogel strength. The printing times for the gripper, linear actuator structure, and compound structure were 27 min, 2 h 25 min, and 5 h 49 min respectively. Immediately following printing, the components were incubated in the printing wells at room temperature for 60 min (Fig. 1B). The wells were then transferred to a watertight container with 2.5% (w/v) CaCl_2 solution and incubated in a 37 °C water bath for 60 min for slurry liquefaction and part retrieval (Fig. 1C) as described previously [15]. Subsequently, the printed alginate components were transferred to a fresh 2.5% (w/v) CaCl_2 solution and incubated overnight at room temperature (Fig. 1D).

2.4 Interfacing FRESH-Printed Alginate Components with External Pressure Control and Measurement Systems

After cross-linking, the structure's base was adhered to a 5 mm thick silicone block for handling and subsequent interfacing with an external pressure control system using Loctite. To create the interface, a pin was first used to penetrate the silicone and actuator membrane. The pin was removed, and a blunt-tipped G25 needle was inserted through the opening and held in place by the silicone block. A 3 mm diameter PTFE tube was connected to the interface needle on one end and a 5 ml syringe on the other. Pressurization of the control line was performed by manually withdrawing and infusing fluid into the printed structure. While this proof-of-concept study did not fully characterize the maximum pressure withstood by the system, previous experiments [15] have demonstrated that the working pressure of the gripper bellows falls between 0.1 and 0.14 kPa. The pressurization of the system was measured with the use of an in-line Microfluidic Sensor Reader (Elveflow) with an acquisition sampling rate of up to 100 Hz and a 11 bit resolution. Data was tracked and analyzed using Elveflow Sensor Interface software.

2.5 Design and Testing of FRESH-Printed Channels for Fluid Routing

To fabricate larger, composite alginate robot structures in which actuators can be individually controlled without external tubing impeding robot motion, fluidic routing channels within the structure are needed. To identify appropriate dimensions for channels using the printer, ink, and printing parameters described above, we fabricated fluidic channel test blocks (Fig. 3A) with both straight (180°) and angled (90°) channels at five diameters: 0.7, 0.85, 1, 1.25, and 1.5 mm. Channels were tested by interfacing a G25 needle with one end and slowly injecting 2.5% w/v CaCl_2 dyed with red glycerin while monitoring the structure with a Canon EOS Rebel T7 camera.

2.6 Design and Testing of a FRESH-Printed Alginate Robot Arm

A soft, multi-actuator robot arm and end effector were created by incorporating the components developed by Sun et al. [15] and the FRESH-printed channels described above (Fig. 2A, B, C, D). The arm is composed of a base, with three parallel linear actuators to provide four degree-of-freedom positioning (Fig. 2E, F, G), a FRESH-printed channel to bring fluid to the end effector for separate control (Fig. 2H), and a soft grasper (Fig. 2I). To achieve watertightness for all actuators and channels, slicing parameters and printing orientation was critical. The hydrogel filament deposition was designed to progress along the axial direction of the arm during printing. The wall thickness for all bellows structures was set to 600 μm , and the inner face of the gripper was printed with a wall thickness of 700 μm in the slicing program. The fluid channel for gripper control was printed along the central axis of symmetry of the three linear actuators with a channel diameter of 2 mm and wall thickness of 1.5 mm.

A pilot trial was performed to assess the range of motion, positioning, and grasping capabilities of the proof-of-concept FRESH-printed alginate robot arm. The FRESH-printed structure was mounted to the silicone block as described and secured using Loctite (Fig. 4E). The silicone block was suspended in a 500 mL bath of 2.5% w/v

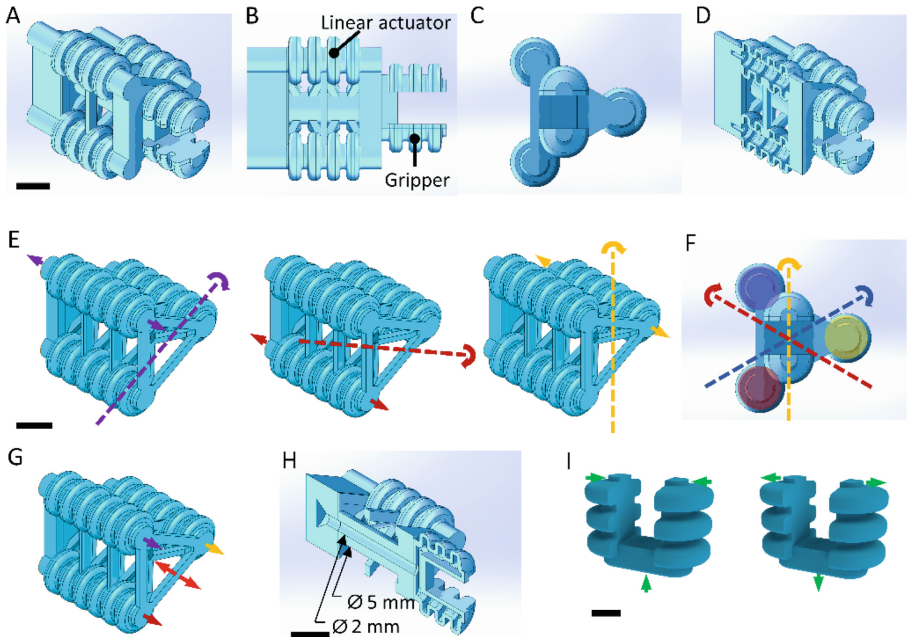


Fig. 2. Soft, multi-actuator robot arm for articulation and grasping. (A) Isometric view of compound structure featuring 3 linear truss actuators, internal routing channels, and distal single-channel gripper. (B) Side view of the compound structure. (C) Top view of the compound structure. (D) Cross-sectional of compound structure highlighting hollow bellows of linear actuators. Scale bar: 5 mm. (E) Isometric model of multi-actuator truss component demonstrating 3 rotational degrees of freedom. The axis of rotation achieved by pressurizing an individual linear actuator is denoted in like colors. Scale bar: 5 mm. (F) Rotational degrees of freedom overlaid on the top-down view of the structure. (G) Isometric model of multi-actuator truss component demonstrating 1 translational degree of freedom by actuating all linear bellows together. (H) Cross-sectional view of compound structure highlighting FRESH-printed channel enabling hydraulic actuation of distal structures. Internal channel diameter of 2 mm. Outer column diameter of 5 mm. Scale bar: 5 mm. (I) Isometric model of single channel gripper component. During infusion, the gripper jaws will bend in (left), and during withdrawal, they will bend out (right). Scale bar: 2 mm. (Color figure online)

CaCl₂ from a wire frame so that the structure could move freely in the solution (see supplemental materials). A G25 blunt-tipped needle was inserted directly into each linear actuator using the interface methods described above. For the gripper actuation line, a G25 needle was inserted into the base of the structure only until it penetrated the funnel-shaped chamber leading to the embedded channel (Fig. 2G). We first tested and measured the range of motion of the entire structure by manually pressurizing the linear actuator control lines independently and monitoring with a Canon EOS Rebel T7 camera. We then tested the grasping ability of the gripper by manually oscillating pressure from the open to the closed position. To demonstrate the strength and stability of the robot arm, we manually positioned various objects within the grasping range of the open gripper and pressurized the system to grasp and hold the object securely. When

a secure grip was established, the linear actuators were again manually pressurized to move the entire arm and transport the object.

3 Results and Discussion

3.1 FRESH-Printed Channels Successfully Transport Fluid Through Alginate Structures

To investigate the potential use of embedded channels in the fabrication of larger, complex alginate robots with distal actuation mechanisms, we fabricated fluidic channel test blocks (Fig. 3A). The dyed CaCl_2 solution was injected into both the straight and bent FRESH-printed channels at all diameters. Fluid successfully passed through the channels without rupturing the surrounding structure, demonstrating consistent flow at diameters larger than 1 mm. There was no observable qualitative difference between the fluid flow passing through the straight and bent channels, suggesting that a range of geometries and pathways are possible for the transport of fluid through alginate structures. The channels continued to function even after repeated injections with no signs of degradation or wear to the channel walls. The main limitation of the direct needle interface is that the repeated insertion of the needle will eventually cause damage to the inlet of the printed channel. Reduced contact between the needle and the internal channel walls improves the life of the printed part. This was implemented in the design of the compound structure by incorporating a hollow chamber within the base block into which the needle may be inserted. Fluid in this chamber is funneled into the smaller channel, rather than having the needle directly contact the internal walls of the channel. Further studies should investigate the impact of channel diameter, length, and path geometry on the laminar flow of hydraulic fluid. Consideration should also be given to the effect that high pressure flow has on the walls of the surrounding structures to determine if shear stress and pressure are a limiting factor to what can be achieved with FRESH-printed channels in alginate robots. As a proof-of-concept, this method of FRESH-printing fluid channels eliminates the need for externally tethered interfaces and enables the actuation of distal components on complex alginate robots.

3.2 Compound FRESH-Printed Structure for Articulation and Grasping

After demonstrating the capability of FRESH-printed channels to transport fluid through alginate structures, we designed and tested a proof-of-concept robot arm comprised of a linear truss structure and a distal gripper. The resulting structure was 20.33 mm \times 22.34 mm \times 31.05 mm and weighed 2.05 g. The actuation of the linear truss elements was achieved through a direct needle interface, while the distal gripper was actuated through a channel running from the base of the structure through a central support column (Fig. 2G). The FRESH-printed robot arm successfully deflected the structure in 4 degrees of freedom with a maximum deflection angle of approximately 25° ($\pm 1^\circ$) from the central axis (Fig. 4A). Future experiments should more specifically quantify independent gripper deflection, maximum linear actuator extension, and the motion of the arm in 3D space.

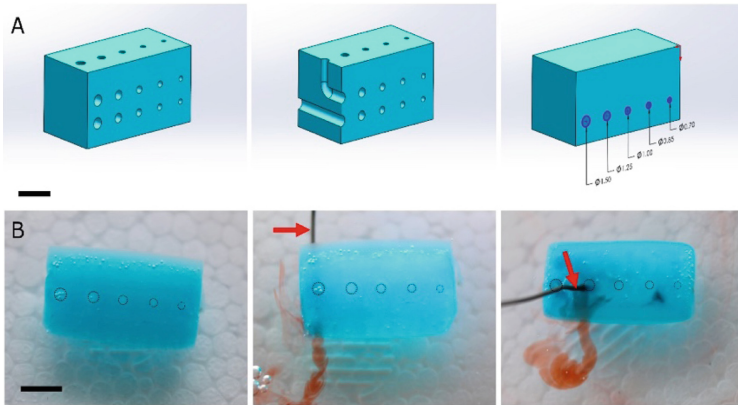


Fig. 3. Schematic of functional microfluidics channels embedded in a 3D FRESH-printed block. (A) Isometric CAD model view of test block with a series of embedded microfluidics channels (left), cross sectional view of 180° and 90° bend internal channels (middle), and dimensioned view of a range of channel diameters (right). Scale bar: 5 mm. (B) Top view of FRESH-printed test block (left), demonstration of dyed fluid flow through 180° channel (middle), and demonstration of dyed fluid flow through 90° bend channel (right). Red arrows indicate the G25 needle which has been interfaced with the channel. Scale bar: 5 mm. (Color figure online)

The robot arm was also capable of controlled grasping through the opening and closure of the distal gripper (Fig. 4B). Articulation and grasping were performed repeatedly in aquatic conditions; the arm manipulated multiple small objects within the environment. Previous experiments have tested the strength of the gripper by securely holding an M3 nut weighing 0.11 g [15]. We repeated this action with the compound arm to demonstrate that there has been no qualitative functionality lost in terms of grip strength (Fig. 4C) and that the arm can sustain a grip on objects at least 5% of its own weight. Future experiments will further validate this by performing force or pressure measurements and comparing to literature values [15].

The combined capabilities of the multi-actuator truss and gripper elements of this structure allow for the robot arm to interact with its environment and perform tasks, including picking up, transporting, and releasing small objects (Fig. 4D). Additional video of articulation and grasping performed by the robot arm are available in the supplemental materials. While the arm performed well in the aqueous environment when removed from the solution and held in air, it was unable to support its own weight and buckled (Fig. 4E). This observation supports what previous reports have established; the unfavorable mechanical properties of alginate-based hydrogels prevent long-term functionality external to an aqueous environment [15]. Articulation and grasping in air and interaction with larger and heavier objects in solution may be more achievable by introducing fiber reinforcements and composite materials to improve the structure's mechanical properties [15, 17, 29, 33].

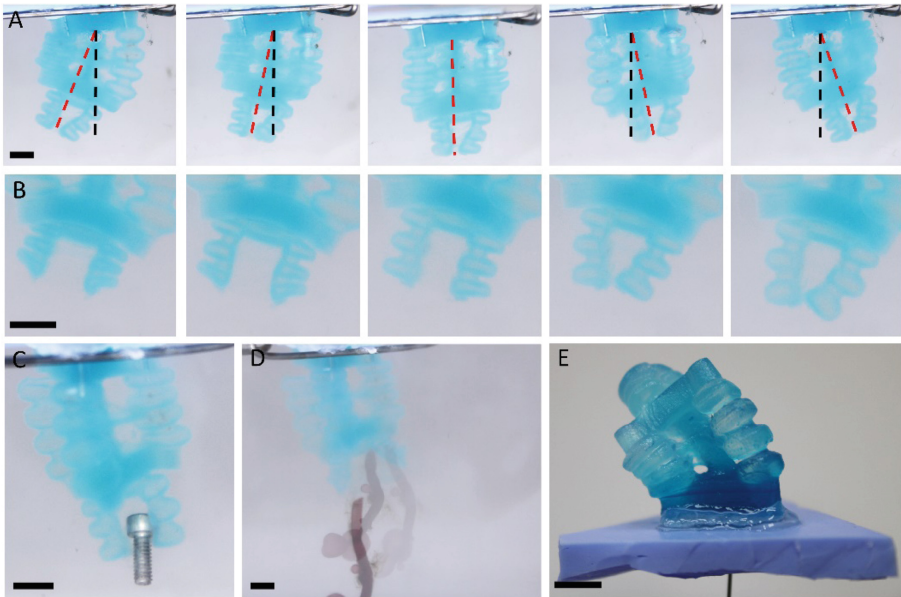


Fig. 4. FRESH-printed robot arm demonstrating complex articulation and grasping. (A) Actuation of the FRESH-printed robot arm produces deflection to the left and right. Scale bar: 5 mm. (B) Actuation of the distal gripper between open and close from left to right. Scale bar: 5 mm. (C) FRESH-printed robot arm securely grasping M3 screw. Scale bar: 5 mm. (D) Actuation of FRESH-printed robot arm allows for the interaction and manipulation of objects within the aquatic environment. Scale bar: 5 mm. (E) FRESH-printed robot arm adhered to silicone block while external to the aqueous environment. Scale bar: 5 mm.

4 Conclusion

Here we presented a proof-of-concept for embedding fluidic channels within alginate structures using FRESH-printing methods to enable the fabrication of multi-actuator robots. The complex actions and tasks performed by the robot arm in this work would not be possible without the combined capabilities of both the linear actuator truss structure and the inclusion of an independently controlled distal gripping mechanism. The functionality of the gripper specifically is enabled by the introduction of embedded FRESH-printed channels to transport hydraulic fluid from the needle interface point to the point of actuation. This reduces the need for externally tethered lines which cause detrimental drag forces and can hinder movement or damage the structure. The functionality of this printed structure suggests that increasingly complex and larger robot limbs can be fabricated using this method without as many challenges typically associated with the scaling of soft hydrogel parts. These findings help to further advance the potential future use of soft biodegradable actuators in marine ecosystems as non-disruptive exploratory robots.

Acknowledgements. This research was supported in part by grants from the NSF DBI 2015317 as part of the NSF/CIHR/ DFG/FRQ/UKRI-MRC Next Generation Networks for Neuroscience

Program, the Presidential Fellowship in the College of Engineering at Carnegie Mellon University, the Collaborative Fellowship from the Department of Mechanical Engineering at Carnegie Mellon University, and funding award no. HQ00342110020 from the National Defense Education Program. Manuscript copy-editing for clarity and grammar after initial drafting was assisted by Grammarly. All edited content was reviewed by the authors.

Supporting Information. Supporting information including supplemental videos and slicer configuration profiles is available online.

References

1. Laschi, C., Mazzolai, B., Cianchetti, M.: Soft robotics: technologies and systems pushing the boundaries of robot abilities. *Sci. Robot.* **1**(1) (2016)
2. Webster-Wood, V.A., et al.: Organismal engineering: toward a robotic taxonomic key for devices using organic materials. *Sci. Robot.* **2**(12) (2017). <https://doi.org/10.1126/scirobotics.aap9281>
3. Kim, J., Park, J., Lee, J.: Biohybrid microsystems actuated by cardiomyocytes: microcantilever, microrobot, and micropump. In: *IEEE International Conference on Robotics and Automation*, Pasadena, CA (2008)
4. Legant, W.R., Pathak, A., Yang, M.T., Deshpande, V.S., McMeeking, R.M., Chen, C.S.: Microfabricated tissue gauges to measure and manipulate forces from 3D microtissues. *Proc. Natl. Acad. Sci. U.S.A.* **106**, 10097–10102 (2009)
5. Holley, M.T., Nagarajan, N., Danielson, C., Zorlutuna, P., Park, K.: Development and characterization of muscle-based actuators for self-stabilizing swimming biorobots. *Lab Chip* **16**, 3473–3484 (2016)
6. Williams, B.J., Anand, S.V., Rajagopalan, J., Saif, M.T.A.: A self-propelled biohybrid swimmer at low Reynolds number. *Nat. Commun.* **5**, 3081 (2014)
7. Nawroth, J.C., et al.: A tissue-engineered jellyfish with biomimetic propulsion. *Nat. Biotechnol.* **30**, 792–797 (2012)
8. Paschal, T., Bell, M.A., Sperry, J., Sieniewicz, S., Wood, R.J., Weaver, J.C.: Design, fabrication, and characterization of an untethered amphibious sea urchin-inspired robot. *IEEE Robot. Autom. Lett.* **4**(4), 3348–3354 (2019)
9. Hwang, J., Wang, W.D.: Shape memory alloy-based soft amphibious robot capable of seal-inspired locomotion. *Adv. Mater. Technol.* **7**(6) (2022). ISSN: 2365709X. <https://doi.org/10.1002/admt.202101153>
10. Ren, K., Yu, J.: Research status of bionic amphibious robots: a review. *Ocean Eng.* **227** (2021). <https://doi.org/10.1016/j.oceaneng.2021.108862>
11. Milana, E., Raemdonck, B.V., Cornelis, K., et al.: EELWORM: a bioinspired multimodal amphibious soft robot. *IEEE Xplore* (2020). <https://doi.org/10.1109/RoboSoft48309.2020.9115989>
12. Inoue, N., Shimizu, M., Hosoda, K.: Self-organization of a joint of cardiomyocyte-driven robot. In: Duff, A., Lepora, N.F., Mura, A., Prescott, T.J., Verschure, P.F.M.J. (eds.) *Biomimetic and Biohybrid Systems. Living Machines 2014*. LNCS, vol. 8608, pp. 402–404. Springer, Cham (2014). https://doi.org/10.1007/978-3-319-09435-9_43
13. Webster, V.A., Hawley, E.L., Akkus, O., Chiel, H.J., Quinn, R.D.: Effect of actuating cell source on locomotion of organic living machines with electrocompact collagen skeleton. *Bioinspir. Biomim.* **11**, 036012 (2016)

14. Hao, Y., Wang, T., Ren, Z., et al.: Modeling and experiments of a soft robotic gripper in amphibious environments. *Int. J. Adv. Robot. Syst.* **14**(3) (2017). ISSN: 17298814. <https://doi.org/10.1177/1729881417707148>
15. Sun, W., et al.: Biodegradable, sustainable hydrogel actuators with shape and stiffness morphing capabilities via embedded 3D printing. *Under Rev.* (2023). Pre-print embargoed until 6/1/2023
16. Baines, R.L., Booth, J.W., Fish, F.E., Kramer-Bottiglio, R.: Toward a bio-inspired variable-stiffness morphing limb for amphibious robot locomotion. In: *IEEE International Conference on Soft Robotics, RoboSoft 2019*, pp. 704–710 (2019)
17. Sun, W., Schaffer, S., Dai, K., Yao, L., Feinberg, A., Webster-Wood, V.: 3D printing hydrogel-based soft and biohybrid actuators: a mini-review on fabrication techniques, applications, and challenges. *Front. Robot. AI* (2021). <https://doi.org/10.3389/frobt.2021.673533>
18. Clause, A.G., Celestian, A.J., Pauly, G.B.: Plastic ingestion by freshwater turtles: a review and call to action. *Sci. Rep.* **11**(1), 5672 (2021). <https://doi.org/10.1038/s41598-021-84846-x>
19. Nelms, S.E., et al.: Plastic and marine turtles: a review and call for research. *ICES J. Mar. Sci.* **73**(2), 165–181 (2016). <https://doi.org/10.1093/icesjms/fsv165>
20. Meaza, I., Toyoda, J.H., Wise J.P.: Microplastics in sea turtles, marine mammals and humans: a one environmental health perspective. *Front. Environ. Sci.* **8** (2021). <https://doi.org/10.3389/fenvs.2020.575614>
21. Ryan, P.G.: Ingestion of plastics by marine organisms. In: Takada, H., Karapanagioti, H.K. (eds.) *Hazardous Chemicals Associated with Plastics in the Marine Environment*. THEC, vol. 78, pp. 235–266. Springer, Cham (2016). https://doi.org/10.1007/698_2016_21
22. Hecht, H., Srebniak, S.: Structural characterization of sodium alginate and calcium alginate. *Biomacromol* **17**(6), 2160–2167 (2016). <https://doi.org/10.1021/acs.biomac.6b00378>
23. Kheirikhah, M.M., Rabiee, S., Edalat, M.E.: A review of shape memory alloy actuators in robotics. In: Ruiz-del-Solar, J., Chown, E., Plöger, P.G. (eds.) *RoboCup 2010: Robot Soccer World Cup XIV*. LNCS, vol. 6556, pp. 206–217. Springer, Heidelberg (2011). https://doi.org/10.1007/978-3-642-20217-9_18
24. Lendlein, A., Gould, O.E.: Reprogrammable recovery and actuation behaviour of shape-memory polymers. *Nat. Rev. Mater.* **4**, 116–133 (2019)
25. Youn, J.-H., et al.: Dielectric elastomer actuator for soft robotics applications and challenges. *Appl. Sci.* **10**, 640 (2020)
26. Polygerinos, P., et al.: Soft robotics: review of fluid-driven intrinsically soft devices; manufacturing, sensing, control, and applications in human-robot interaction. *Adv. Eng. Mater.* **19**, 1700016 (2017)
27. Shin, S.R., et al.: Electrically driven microengineered bioinspired soft robots. *Adv. Mater.* **30**, 1704189 (2018)
28. Hinton, T.J., et al.: Three-dimensional printing of complex biological structures by freeform reversible embedding of suspended hydrogels. *Sci Adv.* **1**, 1–10 (2015). <https://doi.org/10.1126/sciadv.1500758>
29. Sun, W., Tashman, J.W., Shiowski, D.J., Feinberg, A., Webster-Wood, V.: Long-fiber embedded hydrogel 3D printing for structural reinforcement. *ACS Bio-Mater. Sci. Eng.* **8**(1), 303–313 (2022)
30. Lee, A., et al.: 3D bioprinting of collagen to rebuild components of the human heart. *Science* **365**(6452), 482 (2019)
31. Mirdamadi, E., Tashman, J.W., Shiowski, D.J., Palchesko, R.N., Feinberg, A.W.: Emergence of FRESH 3D printing as a platform for advanced tissue biofabrication. *ACS Biomater. Sci. Eng.* **5**, 010904 (2020)
32. Won, P., Ko, S.H., Majidi, C., W. Feinberg, A., Webster-Wood, V.: Biohybrid actuators for soft robotics: challenges in scaling up. *Actuators* **9**, 96 (2020). <https://doi.org/10.3390/act9040096>

33. Patterson, Z.J., Sabelhaus, A.P., Chin, K., Hellebrekers, T., Majidi, C.: An untethered brittle star-inspired soft robot for closed-loop underwater locomotion. In: 2020 IEEE/RSJ International Conference on Intelligent Robots and Systems, pp. 8758–8764 (2020)
34. Patel, D.K., et al.: Highly dynamic bistable soft actuator for reconfigurable multimodal soft robots. *Adv. Mater. Technol.* **8**(2), 2201259 (2023)